Home   Search   Collections   Journals   About   Contact us   My IOPscience

A computational method for the inversion of wide-band GPR measurements

You may also be interested in:

A MODERATE-RESOLUTION, WIDE-BAND, ASTRONOMICAL ECHELLE SPECTROGRAPH.
D. Bardas

Electronics of thin layers of wide-band polymers
Aleksey N Lachinov and Natal'ya V Vorob'eva

Wide-band Multi-layer Ultrasonic Transducers Made of Piezoelectric Films of Vinylidene
Fluoride-Trifluoroethylene Copolymer
Kousaku Sakaguchi, Takashi Sato, Kiyohito Koyama et al.

Analysis of Reflective Part with Wide-Band Property in Single Gap Transflective Fringe-Field
Switching Mode
Jun Baek Park, Hyang Yul Kim, Youn Hak Jeong et al.

High-Speed Mechanical Actuator for Precision Optical Path Length Control
Kosuke Machida, Shigenori Moriwaki and Norikatsu Mio

Wide-Band and Low-Loss Unidirectional SAW Filter
Jum Yamada, Yuuji Fujita and Akitsuna Yuhara

A computational method for the inversion of wide-band GPR measurements

M Salucci[1,2]**, L Tenuti**[2]**, L Poli**[2]**, G Oliveri**[1,2] **and A Massa**[1,2]
[1] ELEDIA@L2S - Laboratoire des Signaux et Systèmes, UMR8506
(CNRS - CS - UPS), 3 rue Joliot-Curie, 91192 Gif-sur-Yvette, France
[2] ELEDIA@UniTN - University of Trento, Via Sommarive 9, I-38123 Trento, Italy
E-mail: andrea.massa@l2s.centralesupelec.fr

Abstract. An innovative method for the inversion of ground penetrating radar (GPR) measurements is presented. The proposed inverse scattering (IS) approach is based on the exploitation of wide-band data according to a multi-frequency (MF) strategy, and integrates a customized particle swarm optimizer (PSO) within the iterative multi-scaling approach (IMSA) to counteract the high non-linearity of the optimized cost function. If from the one hand the IMSA provides a reduction of the ratio between problem unknowns and informative data, on the other hand the stochastic nature of the PSO solver allows to "escape" from the high density of false solutions of the MF-IS subsurface problem. A set of representative numerical results verifies the effectiveness of the developed approach, as well as its superiority with respect to a deterministic implementation.

1. Introduction

In the last decades, there has been a growing interest in developing non-destructive technologies aimed at retrieving an easy-to-interpret image of an inaccessible buried domain [1],[2]. Within this context, the use of ground penetrating radar (GPR) as probing instrument gained particular attention given its robustness and versatility [1]-[7]. Nevertheless, the need for effective computational methods for the inversion of GPR data is still an open issue. Classical microwave tomography techniques introduced for the free-space scenario seem a promising candidate for solving the subsurface inverse scattering (IS) problem. However, suitable extensions of such techniques are needed in order to take into account for the increased complexity of the buried configuration, as well as for the limited amount of information that can be collected by field probes placed only above the interface [2].

When developing GPR microwave techniques, it is worth remarking that an intrinsic frequency diversity is available in the collected measurements thanks to the exploitation of wide-band time-domain pulses, and such a diversity should be regarded as an additional source of information able to mitigate the *ill-posedness* of the subsurface IS problem [3]. As a matter of fact, several approaches able to deal with such wide-band data have been recently proposed, mainly subdivided in (*i*) frequency-hopping (FH) [3],[7] and (*ii*) multi-frequency (MF) [4],[8],[9] strategies. If from the one hand FH-based methods process different samples of the collected GPR spectrum in a cascaded fashion [3], MF-IS techniques exploit the whole data within a single inversion step. According to the reference literature, MF strategies could in principle provide better results than FH-based methods since the joint exploitation of multiple frequencies enlarges the essential dimension of the available data [8]. However, they suffer from an increased complexity of the cost function that has to be minimized in terms of occurrence of local minima, since a larger number of unknowns has to be

retrieved within a single optimization. In such a framework, multi-resolution techniques [3],[9] can be introduced in the inversion scheme to limit the ratio between unknowns and uncorrelated data, by adaptively refining the resolution only within those regions where the targets have been detected. Unfortunately, such approaches only partially solve the problem as they cannot completely prevent local search algorithms from being trapped into false solutions (mathematically represented by local minima of the MF cost function to optimize).

Given all the previous considerations, this work presents an innovative computational method for the inversion of GPR measurements. Such a methodology is based on the integration of the iterative multi-scaling approach (IMSA [9]) and a MF stochastic solver based on the particle swarm optimizer (PSO) [10]-[12]. As shown by a set of representative numerical comparisons, the MF-IMSA-PSO is not only able to provide accurate and robust reconstructions of the buried scenario, but it also significantly overcomes its deterministic counterpart based on a conjugate gradient (CG)-based solver thanks to its increased global convergence capability.

2. Problem formulation and solution approach

Let us consider a standard two-dimensional (2D) GPR prospecting configuration. The upper half-space ($y > 0$) is free-space (ε_0 and σ_0), while the lower half-space ($y < 0$) is occupied by a background medium with complex permittivity equal to $\varepsilon_{eqb}(f) = \varepsilon_{rb}\varepsilon_0 - j\sigma_b/2\pi f$. A buried investigation domain D_{inv} contains an unknown scatterer having relative permittivity and conductivity equal to ε_r^{obj} and σ^{obj}, respectively. D_{inv} is imaged by means of V ideal z-oriented infinite line sources located at constant height above the interface and radiating a wide-band pulse with 3 dB bandwidth covering the interval $[f_{min}, f_{max}]$. Under these hypothesis, the time-domain scattered field collected by M probes co-located with the sources [$\Psi_s^{(v)}(\underline{r}_m^{(v)}, t)$, $v = 1,...,V$, $m = 1,...,M$] is extracted by muting the first temporal interval of the measured total field [3]. Then, after transforming Ψ_s into the frequency-domain, a set of Q frequency samples in the $[f_{min}, f_{max}]$ band are extracted from the computed spectrum

$$E_s^{(v)}\left(\underline{r}_m^{(v)}, f_q\right) = F\left\{\Psi_s^{(v)}\left(\underline{r}_m^{(v)}, t\right)\right\}\bigg|_{f = f_q} \quad v = 1,...,V \quad m = 1,...,M \quad q = 1,...,Q \tag{1}$$

where $F\{a(t)\} = \int_{-\infty}^{+\infty} a(t)\exp(-j2\pi ft)dt$. The q-th sample of E_s is then linked to the unknown total field E_t and to the electromagnetic properties of D_{inv} by means of the non-linear integral *data* equation

$$E_s^{(v)}\left(\underline{r}_m^{(v)}, f_q\right) = \int_{D_{inv}} G_q^{ext}\left(\underline{r}_m^{(v)}, \underline{r}'\right)E_t^{(v)}\left(\underline{r}', f_q\right)\tau\left(\underline{r}', f_q\right)d\underline{r}' \quad v = 1,...,V \quad m = 1,...,M \quad q = 1,...,Q \tag{2}$$

where G_q^{ext} is the *external* Green's function for the half-space scenario and τ is the unknown contrast

$$\tau\left(\underline{r}, f_q\right) = \frac{\varepsilon_{eq}\left(\underline{r}, f_q\right) - \varepsilon_{eqb}\left(f_q\right)}{\varepsilon_0} \quad q = 1,...,Q \quad \underline{r} \in D_{inv} \tag{3}$$

with $\varepsilon_{eq}\left(\underline{r}, f_q\right) = \varepsilon_r(\underline{r})\varepsilon_0 - j\sigma(\underline{r})/2\pi f_q$. Similarly, the incident field for $\underline{r} \in D_{inv}$ is linked to the problem unknowns by means of the *state* equation

$$E_i^{(v)}\left(\underline{r}, f_q\right) = E_t^{(v)}\left(\underline{r}, f_q\right) - \int_{D_{inv}} G_q^{int}\left(\underline{r}, \underline{r}'\right)E_t^{(v)}\left(\underline{r}', f_q\right)\tau\left(\underline{r}', f_q\right)d\underline{r}'$$

$$v = 1,...,V \quad m = 1,...,M \quad q = 1,...,Q \tag{4}$$

where G_q^{int} stands for the *internal* Green's function. Under these hypothesis, in the MF framework the goal of the inverse problem is to find an estimate of E_t and τ inside D_{inv} by finding the global minimum of the following cost function

$$\Phi = \frac{\displaystyle\sum_{m,v,q} \left| E_s^{(v)}\!\left(\underline{r}_m^{(v)}, f_q\right) - \tilde{E}_s^{(v)}\!\left(\underline{r}_m^{(v)}, f_q\right) \right|^2}{\displaystyle\sum_{m,v,q} \left| E_s^{(v)}\!\left(\underline{r}_m^{(v)}, f_q\right) \right|^2} + \frac{\displaystyle\sum_{n,v,q} \left| E_i^{(v)}\!\left(\underline{r}_n, f_q\right) - \tilde{E}_i^{(v)}\!\left(\underline{r}_n, f_q\right) \right|^2}{\displaystyle\sum_{n,v,q} \left| E_i^{(v)}\!\left(\underline{r}_n, f_q\right) \right|^2} \tag{5}$$

where $\tilde{E}_s^{(v)}$ and $\tilde{E}_i^{(v)}$ are the retrieved scattered and incident fields computed through (2) and (4), while N is the number of square basis functions used to discretize D_{inv}. The solution of such a problem is obtained by integrating a customized MF particle swarm optimizer (MF-PSO) within an iterative multi-scaling approach (IMSA) made of S multi-zooming steps as follows:

1. *IMSA Initialization (s = 0).* Subdivide D_{inv} into N square sub-domains;

2. *Low-Resolution Reconstruction.* Minimize Φ in I iterations by means of the MF-PSO:
   a. *Swarm Initialization (i = 0).* Generate a swarm of P particles by initializing their positions as random perturbations of the empty-background configuration and considering random velocities. Towards this end, the following relationship between the contrast at each frequency and at a reference frequency $\overline{f}$ is exploited

$$\tau\!\left(\underline{r}_n, f_q\right) = \mathrm{Re}\!\left\{\tau\!\left(\underline{r}_n, \overline{f}\right)\right\} + j \frac{\overline{f}}{f_q} \mathrm{Im}\!\left\{\tau\!\left(\underline{r}_n, \overline{f}\right)\right\} \quad n = 1,...,N \quad q = 1,...,Q; \tag{6}$$

   b. *Swarm Evaluation.* Compute Φ for each particle and update the global and personal best positions;
   c. *Swarm Updating.* Update the velocity and the position of each particle to make the swarm evolve towards the next iteration ($i = i + 1$);
   d. *PSO Termination.* Stop when a maximum number of iterations I has been reached;

3. *Multi-Resolution Loop (s=2,...,S).* Identify the region of interest $D^{(s)} \subset D^{(s-1)}$ ($D^{(1)} = D_{inv}$) and discretize it into N cells.
   a. *High-Resolution Reconstruction.* Exploit the information collected at the $(s-1)$-th step to initialize the swarm and minimize the cost function through the MF-PSO;
   b. *IMSA Termination.* End the multi-zooming loop once a suitable stopping criterion is met ($s = S$).

3. Numerical results

The goal of this section is to numerically assess the effectiveness and the robustness of the MF-IMSA-PSO when blurring the collected time-domain total field with the desired level of signal-to-noise ratio (SNR). Moreover, its performances will be compared to those of the MF-IMSA-CG, a deterministic implementation exploiting a CG-based MF-IS solver.

3.1. Performance comparison

Let us consider the target in Fig. 1(*a*) (*L-Shaped* profile, $\varepsilon_r^{obj} = 5$ and $\sigma^{obj} = 0.001$ S/m). A square D_{inv} (side 0.8 m) is embedded in a lossy soil with $\varepsilon_{rb} = 4$ and $\sigma_b = 0.001$ S/m, while $V = 10$ sources and $M = 9$ probes are used to image it, by simulating the buried scenario in time-domain by means of the *GPRMax2D* simulator [13]. $Q = 5$ equally-spaced frequency samples are extracted from the collected GPR spectrum in the $[200,600]$ MHz band. Fig. 1(*b*) shows the retrieved profile (at $\overline{f} = 400$

MHz) by the MF-IMSA-PSO when a significant amount of noise is added to the collected *radargram* ($SNR = 20$ dB). As it can be easily observed, the target is correctly localized and shaped, with a good estimation of the contrast. Moreover, the MF-IMSA-PSO significantly outperforms the MF-IMSA-CG, this latter providing a strong under-estimation of the contrast [Fig. 1(*c*) vs. Fig. 1(*b*)].
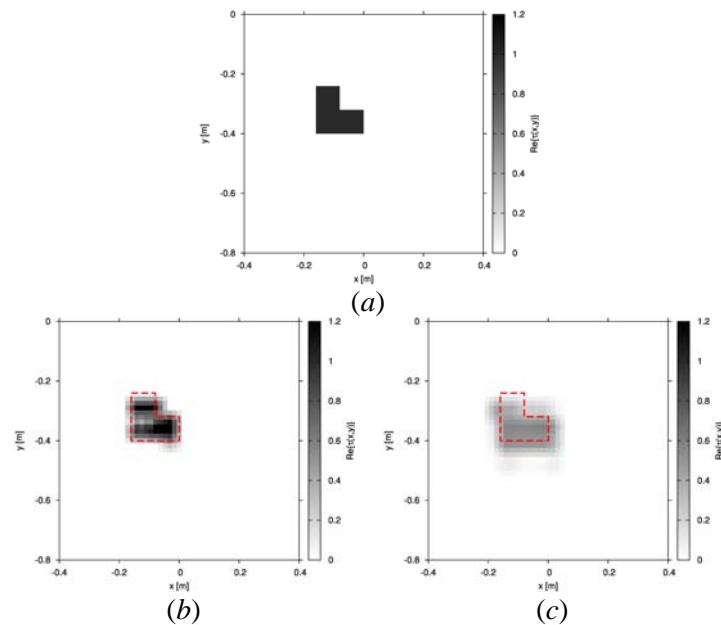

Figure 1. *L-shaped scatterer* - (*a*) Actual dielectric profile and retrieved profiles by (*b*) MF-IMSA-PSO and (*c*) MF-IMSA-CG (*SNR* = 20 dB).

Such a superiority is even more evident for a *I-Shaped* profile [$\varepsilon_r^{obj} = 5$ and $\sigma^{obj} = 0.001$ S/m - Fig. 2(*a*)]. As a matter of fact, the MF-IMSA-CG fails in correctly identifying the support of the target [Fig. 2(*c*)], while a very accurate estimation is provided by the proposed approach [Fig. 2(*b*)].
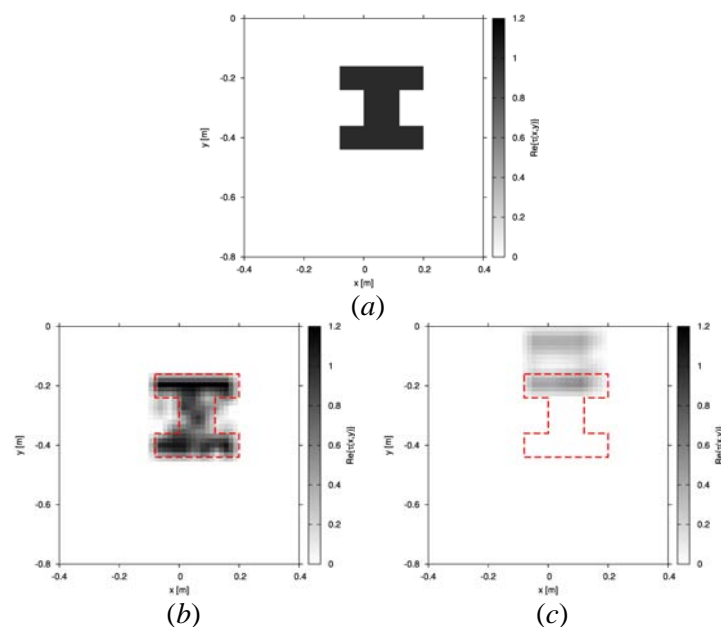

Figure 2. *I-shaped scatterer* - (*a*) Actual dielectric profile and retrieved profiles by (*b*) MF-IMSA-PSO and (*c*) MF-IMSA-CG (*SNR* = 20 dB).

3.2. Circular target at different depths

In order to further investigate the robustness and the effectiveness of the MF-IMSA-PSO, let us consider the retrieval of a circular target ($\varepsilon_r^{obj} = 5$ and $\sigma^{obj} = 0.001$ S/m) buried at different depths inside D_{inv} [$d^{obj} = 0.16$ m - Figs. 3(a),3(b), $d^{obj} = 0.4$ m - Figs. 3(c),3(d) and $d^{obj} = 0.64$ m - Figs. 3(e),3(f)]. As it can be seen from the reported reconstructions on the right column of Fig. 3, the developed methodology is able to correctly locate and shape the target is all cases, even if an unavoidable degradation of the accuracy is observed when increasing the depth of the scatterer inside the lossy background [Fig. 3(f) vs. Fig. 3(b)].
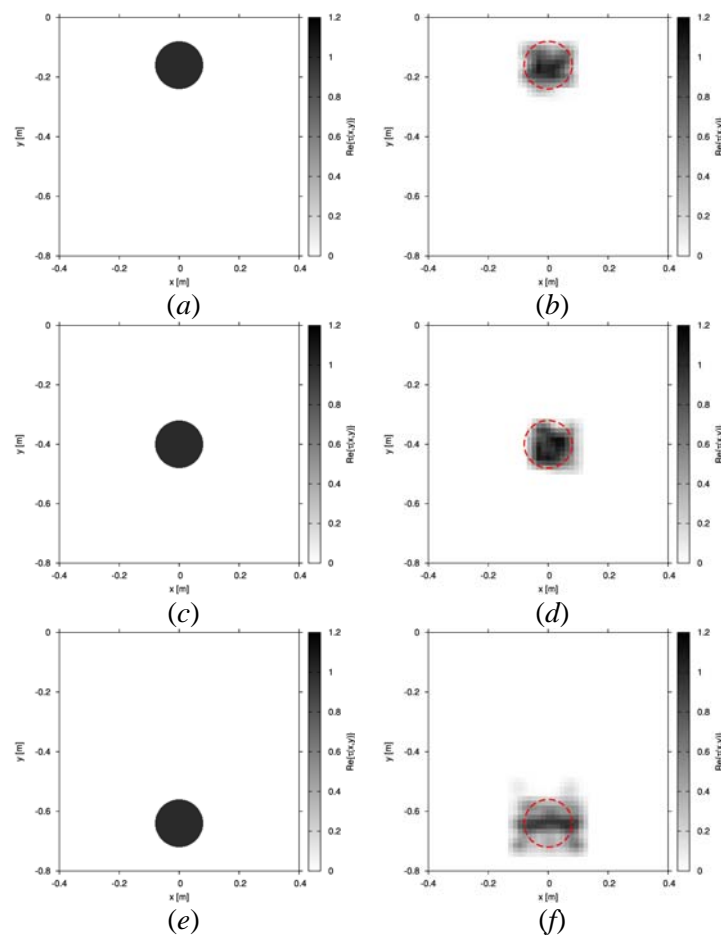

Figure 3. *Circular scatterer* - (*a*)(*c*)(*e*) Actual profiles and (*b*)(*d*)(*f*) MF-IMSA-PSO reconstructions when (*a*)(*b*) $d^{obj} = 0.16$ m, (*c*)(*d*) $d^{obj} = 0.4$ m and (*e*)(*f*) $d^{obj} = 0.64$ m (*SNR* = 40 dB).

4. Conclusions

A new computational method for the inversion of multi-frequency GPR data has been proposed. The MF-IMSA-PSO benefits from a reduction of the ratio between problem unknowns and informative data thanks to the IMSA, while provides robust minimizations of the MF cost function thanks to the *hill-climbing* properties of the employed stochastic optimizer. A set of numerical examples has validated the proposed approach, that showed its superiority over a deterministic CG-based implementation.

References
[1] Lesselier D and Habashy T 2000 Special issue on electromagnetic imaging and inversion on the Earth's subsurface *Inverse Prob.* **16**
[2] Chen C.-C., Johnson J. T., Sato M. and Yarovoy A. G. 2007 Special issue on subsurface sensing using ground-penetrating radar *IEEE Trans. Geosci. Remote Sens.* **45**
[3] Salucci M, Oliveri G and Massa A 2015 GPR prospecting through an inverse scattering frequency-hopping multi-focusing approach *IEEE Trans. Geosci. Remote Sens.* **53** 6573-6592
[4] Persico R, Soldovieri F and Leone G 2006 A microwave tomographic imaging approach for multibistatic configuration: the choice of the frequency step *IEEE Trans. Instrum. Meas.* **55** 1926-1934
[5] Salucci M, Oliveri G, Randazzo A, Pastorino M and Massa A 2014 Electromagnetic subsurface prospecting by a multifocusing inexact Newton method within the second-order Born approximation *J. Opt. Soc. Am. A* **31** 1167-1179
[6] Salucci M, Oliveri G, Randazzo A, Pastorino M and Massa A 2014 Electromagnetic subsurface prospecting by a fully nonlinear multi-focusing inexact Newton method *J. Opt. Soc. Am. A* **31** 2618-2629
[7] Moriyama T, Salucci M, Oliveri G, Tenuti L, Rocca P and Massa A 2014 A Multi-scaling deterministic imaging for GPR survey *Proc. 2014 IEEE Antenna Conf. Ant. Meas. Appl. (Antibes Juan-les-Pins)* 1-3
[8] Bucci O M, Crocco L, Isernia T and Pascazio V 2000 Inverse scattering problems with multifrequency data: reconstruction capabilities and solution strategies *IEEE Trans. Geosci. Remote Sens.* **38** 1749-1756
[9] Franceschini D, Donelli M, Azaro R and Massa A 2007 Dealing with multi-frequency scattering data through the IMSA *IEEE Trans. Antennas Propag.* **55** 2412-2417
[10] Rocca P, Benedetti M, Donelli M, Franceschini D and Massa A 2009 Evolutionary optimization as applied to inverse problems *Inverse Problems* **25** 1-41
[11] Donelli M and Massa A 2005 Computational approach based on a particle swarm optimizer for microwave imaging of two-dimensional dielectric scatterers *IEEE Trans. Microw. Theory Tech.* **53** 1761-1776
[12] Donelli M, Franceschini D, Rocca P and Massa A 2009 Three-dimensional microwave imaging problems solved through an efficient multiscaling particle swarm optimization *IEEE Trans. Geosci. Remote Sens.* **47** 1467-1481
[13] Giannopoulos A 2005 Modelling ground penetrating radar by GprMax *Construct. Build. Mater.* **19** 755 -762